ChemComm

A topological isomer of the Au25(SR)18- nanocluster

Journal:	*ChemComm*
Manuscript ID	CC-COM-05-2020-003334.R1
Article Type:	Communication

Journal Name

COMMUNICATION

A topological isomer of the $Au_{25}(SR)_{18}^-$ nanocluster †

María Francisca Matus[a], Sami Malola[a], Emily Kinder Bonilla,[b] Brian M. Barngrover,[b,c] Christine M. Aikens[b] and Hannu Häkkinen[a,*]

Received 00th January 20xx,
Accepted 00th January 20xx

DOI: 10.1039/x0xx00000x

www.rsc.org/

Energetically low-lying structural isomers of the much-studied thiolate-protected gold cluster $Au_{25}(SR)_{18}^-$ are discovered from extensive (80 ns) molecular dynamics (MD) simulations using the reactive molecular force field ReaxFF and confirmed using the density functional theory (DFT). A particularly interesting isomer is found which is topologically connected to the known crystal structure by a low-barrier collective rotation of the icosahedral Au_{13} core. The isomerization takes place without breaking of any Au-S bonds. The predicted isomer is essentially iso-energetic with the known $Au_{25}(SR)_{18}^-$ structure but has a distinctly different optical spectrum. It has a significantly larger collision cross-section as compared to the known structure, which suggests it could be detectable in gas phase ion-mobility mass spectrometry.

Over the last decade, a remarkable progress has taken place in synthesis, purification and characterization of a new class of atomically precise nanomaterials, the so-called monolayer-protected metal clusters (MPCs) of 1-3 nm metal core size.[1-3] The multitude of sizes, shapes and metal-ligand compositions, as well as various currently known structural motifs of available MPCs lays out an intriguing palette for both experimental and theoretical studies of physicochemical properties of nanoscale metals. The high versatility offered by the surface chemistry, has allowed their extensive exploration in catalysis, sensing, biomedical and electronic applications, to name a few.[1]

MPCs are made through wet-chemistry synthesis by reducing metals salts in the presence of the protecting ligands. Interpretation of the experimental data for their physicochemical properties measured in the solvent (usually around room temperature) relies heavily on state-of-art DFT calculations and on the additional assumption that the atomic structure from single-crystal X-ray diffraction (SCXRD) is the proper structure to be considered as the model for the theoretical work. This approach, while driven by practical considerations in many cases, may miss important effects if the synthesis has produced energetically low-lying structural isomers of a given cluster but the effects of the isomers are not taken into consideration when the data is interpreted.

For metal clusters prepared and analysed in the gas phase, the existence of isomers, influencing the ensemble measurements of all physicochemical properties, has been long recognized. For instance, isomers of small gold cluster anions play an important role for the 2D-3D structural transition around 12-14 atoms and have been detected by ion mobility measurements and by photoelectron spectroscopy, even at relatively low temperatures, below 300 K.[4-6] DFT calculations have been instrumental in predicting the many energetically low-lying isomers of gold clusters and their effects in measured ensemble properties. [5-7] Fluxionality of MgO-supported small gold clusters going dynamically through several isomers while reacting with O_2 and CO has been suggested to lower the critical reaction barriers for CO oxidation.[8]

In the field of MPCs, isolation of cluster isomers followed by a successful structure determination from SCXRD experiments is still quite rare.[9-11] For thiolate-protected gold clusters, the only experimentally demonstrated case of structural isomers is the cluster $Au_{38}(PET)_{24}$ (where PET = phenyl ethyl thiol). The first crystal structure of this cluster was published in 2010[9] and in 2015 a higher-energy isomer was successfully isolated and crystallized.[10] Both structures have an Au_{23} core but its shape as well as the details of the protecting gold-thiolate ligand layer around the core are different. DFT work[12] using various xc functionals as well as very recent Monte Carlo simulations using DFT-based machine learning potentials[13] have investigated the energetics and dynamical stability of the $Au_{38}(SR)_{24}$ isomers.

The $Au_{25}(SR)_{18}^-$ is the most studied thiolate-protected gold cluster up to date. Significant breakthroughs were made when

[a] Departments of Physics and Chemistry, Nanoscience Center, University of Jyväskylä, FI-40014 Jyväskylä, Finland
[b] Department of Chemistry, Kansas State University, Manhattan, KS 66506, USA
[c] Department of Chemistry, Stephen F. Austin State University, Nacogdoches, TX 75962, USA
* hannu.j.hakkinen@jyu.fi

†Electronic Supplementary Information (ESI) available: Details of simulation and analysis methods, parametrization of the ReaxFF force field, Figs. S1-S4, Table S1, video: Au25_isomerization.mp4
See DOI: 10.1039/x0xx00000x

its atomic structure was serendipitously predicted by DFT and determined by SCXRD in 2008,[14-16] although several groups had succeeded in isolating it long before and its chemical composition had been known since 2004[17-19]. The atomic structure found by SCXRD can be concisely described in a "divide-and-protect"[20] notation as $[Au_{13}(ico)@(RS\text{-}Au\text{-}SR\text{-}Au\text{-}SR)_6]^-$, i.e., having an icosahedral Au_{13} core protected by six V-shaped "long" gold-thiolate units. The electronic structure of the cluster is well understood by the "superatom" model which predicts a closed-shell octet configuration by delocalized Au(6s) electrons in the metal core.[7,14,16,21]

While a large amount of the available experimental data on the $Au_{25}(SR)_{18}^-$ anion has been successfully interpreted by building theoretical models based on the known crystal structure with the PET ligand, there have been two theoretical suggestions previously of an alternative arrangement of the gold-thiolate units in the protecting shell. In 2011, Lopez-Acevedo and Häkkinen studied derivatives of the $Au_{25}(SR)_{18}^-$ cluster structure (using a methylthiolate SCH_3 as the model ligand, denoted hereafter as MET). They suggested that an intermediate cluster $Au_{21}(SR)_{14}^-$, which has been consistently seen in the electrospray ionization mass spectrometry (ESI-MS) experiments as a major charged fragment of $Au_{25}(SR)_{18}^-$, could have a structure $[Au_{13}(ico)@(RS\text{-}Au\text{-}SR\text{-}Au\text{-}SR)_2(RS\text{-}Au\text{-}SR)_4]^-$, where the icosahedral Au_{13} re-organizes to accommodate binding of the two sulphur ends of each gold-thiolate unit to nearest-neighbour core Au atoms.[22] Liu et al.[23] observed a similar bonding motif for the $Au_{25}(SR)_{18}^-$ by using the MET as a model ligand as well. It is also interesting that Omoda et al.[24] have suggested, based on spectroscopy data and modelling, an fcc symmetry for the Au_{13} core of an Au_{25} cluster where the ligand was a thiolated glycine.

Comprehensive exploration of phase space becomes critical when mapping potential cluster isomers, and empirical reactive force fields can extend the physical simulation times by several orders of magnitude as compared to DFT-MD. For that reason, we employed the so-called reactive force field (ReaxFF)[25] to run molecular dynamics simulations. A parametrization of ReaxFF reproducing reasonably well the known structures of a few MET-protected (Au_{25}, Au_{38}, Au_{144}) clusters exists in the literature.[26] However, it had not been previously tested with finite-temperature MD simulations. Our initial MD runs around room temperature employing the published parametrization[26] yielded unsatisfactory (unphysical) dynamics in the ligand layer, such as breaking of intramolecular S-C bonds. For that reason, we have used a "re-parametrized" version of the ReaxFF potential (details given in the ESI). We ran MD simulations starting from a model structure $Au_{25}(MET)_{18}$ derived from the experimental crystal structure of $[Au_{25}(PET)_{18}]^-$ (refs 15,16).

We ran three sets of MD runs (20 ns at 200 K, 20 ns at 250 K and 40 ns at 300K) and monitored the radius of gyration R_g (definition given in the ESI) of the cluster. The results are shown in Fig. 1a and b. During the MD runs at 200 K and 250 K, the R_g fluctuates around a well-defined value of about 4.5 Å; however, soon after the system was heated to 300 K, R_g jumps to an intermediate value of about 4.62 Å and reaches then a high value of about 4.95 Å for the remainder of the run. Fig. 1e shows four snapshot structures from the MD runs in the time window of 40 ns to 60 ns. While the cluster mostly vibrates around the equilibrium structure for at 200 K and 250 K (first 40 ns), it transforms first by twisting the $Au_2(SR)_3$ units, followed by re-organization of the whole structure in such a way that most of the gold-thiolate units are bound to nearest-neighbour Au atoms of the core.

For reference, we also ran DFT-MD simulations of $[Au_{25}(MET)_{18}]^-$ but for much shorter times (33 ps). We used elevated temperatures (300, 450, 800 K) in order to speed up exploration of the configuration space. We used the GPAW real-space DFT implementation[27] and the PBE electron exchange-correlation functional [28] (further technical details in the ESI). As seen in Fig. 1c and d, the R_g increases significantly during heating from 450 K to 800 K and fluctuates around 5 Å, similar to cluster dynamics at 300 K observed in the ReaxFF-MD runs.

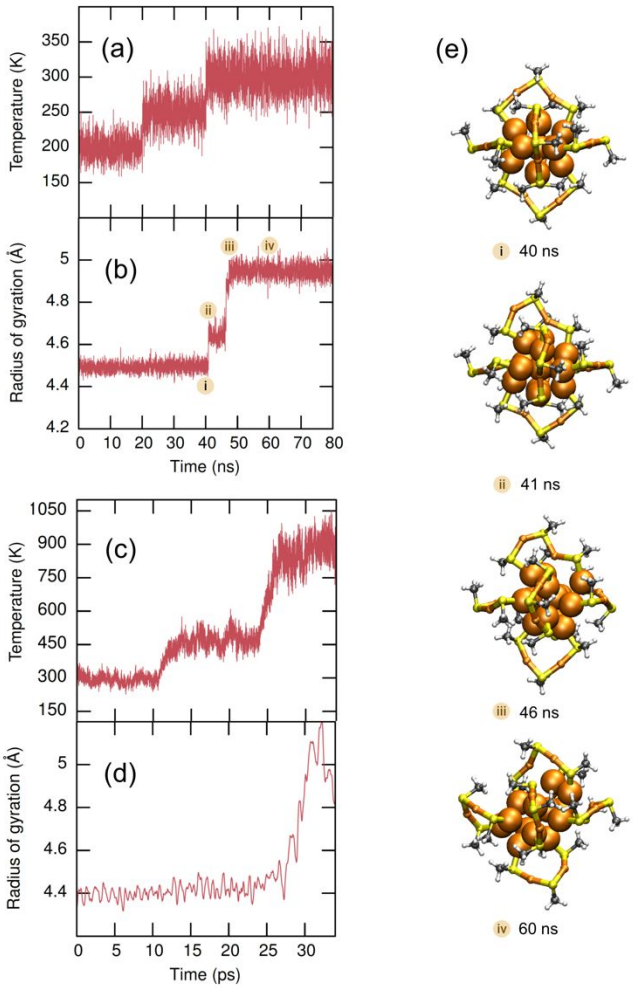

Fig. 1 Time-evolution of (a) temperature and (b) radius of gyration of the $Au_{25}(MET)_{18}$ cluster in ReaxFF-MD runs. For comparison, (c) and (d) show the corresponding data in DFT-MD runs of $[Au_{25}(MET)_{18}]^-$. (e) Four selected snapshots from the ReaxFF-MD runs in the time window of 40-60 ns (300 K) showing the rearrangement of the structure. The Au_{13} core is depicted as spheres and the six RS-Au-SR-Au-SR units with balls and sticks (Au: golden yellow; S: yellow; C: gray; H: white).

Several structures produced by both ReaxFF and DFT MD runs were further analysed by optimizing them to a nearest local energy minimum using DFT. For comparison, we also included model structures based on the reported crystal structures of anionic, neutral and cationic $Au_{25}(PET)_{18}$ (refs. 15,16,29,30) but re-optimized here as anions and by replacing the PET with MET, as well as an isomer of $[Au_{25}(MET)_{18}]^-$ discovered in our previous work.[31]

All the considered structures, labelled as **1** to **32**, are listed in Table S1. All isomer energies were compared to the structure **2** obtained by re-optimizing the crystal structure of the neutral $Au_{25}(PET)_{18}$ cluster as anion.[29] Fig. S1 shows correlation of the "similarity index" and isomer energy. As a "similarity index", we used the distance between a given isomer structure and the reference in a multi-dimensional space, as calculated from the so-called Many-Body Tensor Representation (MBTR).[13,32] MBTR folds all the structural details of a cluster into a 1D vector, which makes it straightforward to compare differences of two structures as the difference norm of the vectors (see details in ESI text). Isomers within 1 eV from the reference are shown in Fig. S2. From Fig. S1 we note that isomers **1, 3 – 8, 13, 14, 16, 19 – 22** and **25** are within 0.3 eV from **2**. Most of them differ from **2** mainly by the small variations in the ligand shell such as rotation of MET groups causing different conformations.

Fig. S1 implies a general positive correlation between the isomer energy and MBTR distance to the reference: isomers that are geometrically close to the reference also have low isomer energy as expected. However, it is very interesting to note that isomers **4** and **25** make an exemption; they have a large MBTR distance but low energy. These isomers have the ligand arrangement discussed previously in refs. 22, 23. They are virtually iso-energetic with **2** within the considered numerical error in energy differences.

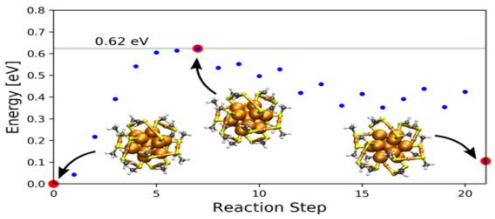

Fig. 2 Energy profile for the isomerization reaction from structure **2** to isomer **4**. The reaction involves a collective rotation of the Au_{13} core and re-organization of the six RS-Au-SR-Au-SR units, with sharpening of the central Au-SR-Au angle changing from 100.7 to 91.6 degree (see also Fig. S3). No Au-SR bonds are broken in this process. The process is also visualized in ESI video 1.

We discovered that isomer **4** is topologically connected to the experimentally known $[Au_{25}(PET)_{18}]^-$ via a simple collective rotation of the Au_{13} core. We performed a series of partially constrained minimizations along the rotation. The energy profile, shown in Fig. 2, implies a very low energy of 0.6 eV for this process. It is notable that no Au-S bonds need to break in this transformation which is the key to the low barrier. This process resembles partially the predicted reversal of handedness for the chiral $Au_{38}(MET)_{24}$ cluster[31] (see also ESI video 1).

Could the predicted isomer **4**, shown here to be essentially iso-energetic and topologically connected to the known structure of $[Au_{25}(PET)_{18}]^-$, be detected under suitable experimental conditions? Our DFT calculations indicate that the electronic structure of isomer **4**, re-optimized with the PET ligand, features a significantly larger HOMO-LUMO energy gap and vertical electron binding energy (1.88 eV and 3.76 eV) as compared to $[Au_{25}(PET)_{18}]^-$ crystal structure (1.20 eV and 3.23 eV, see Fig. S4). The calculated UV-vis optical absorption spectrum reflects the larger optical gap of the isomer and a distinct peak at about 450 nm (Fig. 3a). As Fig. 3b shows, modelling an ensemble absorption spectrum produced by a possible 1:1 or 2:1 mixtures of GS:4 is still consistent with the experimental data.[15,16] This implies that existence of the isomer **4** is not ruled out by the existing experimental UV-vis solution data. Regarding the absence of isomer **4** in the current SCXRD data, one could speculate that the number and type of co-crystallization solvent molecules may play a pivotal role in this matter. Even if the known structure and isomer **4** would be present in equal amounts in solution after synthesis, cluster-counterion interactions under crystallization conditions may not be favourable for formation of high-quality single crystals of isomer **4**. This may explain why this structure has not yet been discovered in the crystalline state.

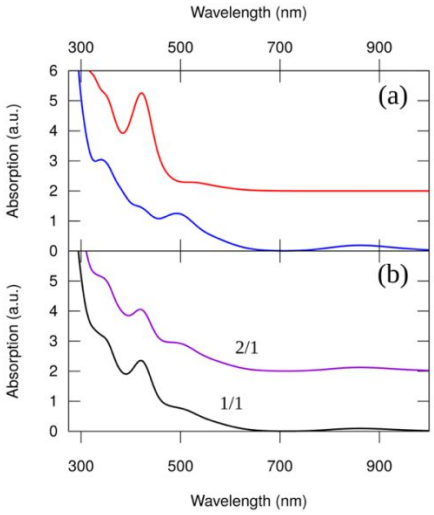

Fig. 3 (a) Calculated UV-vis absorption spectra of the crystal structure (blue curve) and isomer **4** (red curve) of $[Au_{25}(PET)_{18}]^-$, (b) Ensemble spectra of the data shown in (a) with 1/1 and 2/1 ratios of the crystal structure/isomer.

To this end, we expect that the existence of isomer **4** (and other potential low-energy isomers) might be better manifested in gas-phase experiments. It is exciting to note that gas-phase characterization of both structural and electronic properties of anionic ligand-protected gold and silver clusters is now becoming feasible.[33-38] It would be extremely interesting, e.g., to re-analyse the measured photoelectron detachment data from $[Au_{25}(SC_{12}H_{25})_{18}]^-$ (ref. 32) by taking into account possible effects from isomers discussed in this work. Another promising method might be combined mass/mobility measurements that yield information about the collision cross-section ("geometrical cluster size") with the carrier gas molecules.[6] We predict that the collision cross-section of

isomer **4** modelled with PET ligand is significantly larger than that of any known $[Au_{25}(SR)_{18}]^q$ (q=+,0,-) structure (Fig. 4) and should clearly show up as a separate peak in the analysis. This prediction calls for re-analysis of a rather old time of flight data[39] of $[Au_{25}(PET)_{18}]^-$ and motivates new measurements for collision cross-sections. Gas-phase characterizations of $[Au_{25}(SR)_{18}]^-$ clusters made with short alkylthiols[40] would be intriguing as well.

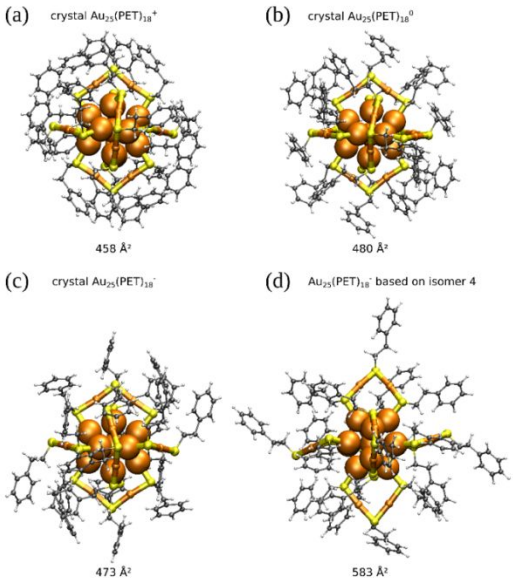

Fig. 4 Calculated collision cross-section for the experimental crystal structure of (a) $[Au_{25}(PET)_{18}]^+$, (b) $[Au_{25}(PET)_{18}]^0$, (c) $[Au_{25}(PET)_{18}]^-$ and for (d) the model structure of $[Au_{25}(PET)_{18}]^-$ based on the PBE-relaxed geometry of isomer **4**.

This work was supported by the Academy of Finland (grants 292352 and 319208) and by the US National Science Foundation (grant CHE-1213771). The computations were made at the JYU node of the FGCI infrastructure and as part of the PRACE project 2018194723 in the Barcelona Supercomputing Center. Reparameterization of the ReaxFF was performed on the Beocat supercomputer at KSU, supported in part by NSF Grants CHE-1726332, CNS-1006860, EPS-1006860, and EPS-0919443. We thank A. Pihlajamäki, E. Kalenius and T. Buergi for discussions.

Conflicts of interest

There are no conflicts to declare.

Notes and references

1 T. Tsukuda and H. Häkkinen, *Protected Metal Clusters: From Fundamentals to Applications*, Elsevier, Amsterdam, 2015.
2 A. Fernando, K.L.D.M. Weerawardene, N.V. Karimova, C.M. Aikens, *Chem. Rev*., 2015, **115**, 6112.
3 R. Jin, C. Zheng, M. Zhou and Y. Chen, *Chem. Rev*., 2016, **116**, 10346.
4 H. Häkkinen, M. Moseler and U. Landman, *Phys. Rev. Lett*., 2002, **89**, 033401.
5 H. Häkkinen, B. Yoon, U. Landman, X. Li, H.J. Zhai and L.S. Wang, *J. Phys. Chem. A,* 2003, **107**, 6168.
6 F. Furche, R. Ahlrichs, P. Weis, C. Jacob, S. Gilb, T. Bierweiler and M. Kappes, *J. Chem. Phys*., 2002, **117**, 6982.
7 H. Häkkinen, *Chem Soc. Rev*., 2008, **37**, 1847.
8 H. Häkkinen, S. Abbet, A. Sanchez, U. Heiz and U. Landman, *Angew. Chem. Int. Ed*., 2003, **42**, 1297.
9 H. Qian, W.T. Eckenhoff, Y. Zhu, T. Pintauer and R. Jin, *J. Am. Chem. Soc.*, 2010, **132**, 8280.
10 S. Tian, Y.Z. Li, M.B. Li, J. Yuan, J. Yang, Z. Wu and R. Jin, *Nat. Comm.,* 2015, **6**, 8667.
11 Z.-J. Guan, F. Hu, J.-J. Li, Z.-R. Wen, Y.-M. Lin and Q.-M. Wang, *J. Am. Chem. Soc.*, 2020, **142**, 2995.
12 R. Juarez-Mosqueda, S. Malola and H. Häkkinen, *Eur. Phys. J. D,* 2019, **73**, 62.
13 A. Pihlajamäki, J. Hämäläinen, J. Linja, P. Nieminen, S. Malola, T. Kärkkäinen and H. Häkkinen*, J. Phys. Chem*., 2020, *In Revision.*
14 J. Akola, M. Walter, R.L. Whetten, H. Häkkinen and H. Grönbeck, *J. Am. Chem. Soc.,* 2008, **130**, 3756.
15 M.W. Heaven, A. Dass, P.S. White, K.M. Holt and R.W. Murray, *J. Am. Chem. Soc*., 2008, **130**, 3754.
16 M. Zhu, C.M. Aikens, F.J. Hollander, G.C. Schatz and R.C. Jin, *J. Am. Chem. Soc*., 2008, **130**, 5883.
17 J.F. Parker, C.A. Fields-Zinna and R.W. Murray, *Acc. Chem. Res*., 2010, **43**, 1289.
18 Y. Negishi, Y. Takasugi, S. Sato, H. Yao, K. Kimura and T. Tsukuda, *J. Am. Chem. Soc*., 2004, **126**, 6518.
19 T.G. Schaaff and R.L. Whetten, *J. Phys. Chem. B*, 2000, **104**, 2630.
20 H. Häkkinen, M. Walter and H. Grönbeck, *J. Phys. Chem. B*, 2006, **110**, 9927.
21 M. Walter, J. Akola, O. Lopez-Acevedo, P.D. Jadzinsky, G. Calero, C.J. Ackerson, R.L. Whetten, H. Grönbeck and H. Häkkinen, *Proc. Natl. Acad. Sci USA*, 2008, **105**, 9157.
22 O. Lopez-Acevedo and H. Häkkinen, *Eur. Phys. J. D*, 2011, **63**, 311.
23 C. Liu, S. Lin, Y. Pei and X.C. Zeng, *J. Am. Chem. Soc.*, 2013, **135**, 18067.
24 T. Omoda et al., *J. Phys. Chem. C*, 2018, **122**, 13199.
25 A. C. T. Van Duin, S. Dasgupta, F. Lorant and W. A. Goddard, *J. Phys. Chem. A*, 2001, **105**, 9396.
26 G.T. Bae and C.M. Aikens, *J. Phys. Chem. A*, 2013, **117**, 10438.
27 J. Enkovaara *et al*., *J. Phys. Cond. Matt*., 2010, **22**, 253202.
28 J.P. Perdew, K. Burke and M. Ernzerhof, *Phys. Rev. Lett*., 1996, **77**, 3865.
29 M. Zhu, W.T. Eckenhoff, T. Pintauer and R. Jin, *J. Phys. Chem. C*, 2008, **112**, 14221.
30 M.A. Tofanelli, S. Malola, T. Ni, K. Salorinne, B. Newell, B. Phillips, H. Häkkinen and C.J. Ackerson, *Chemical Science,* 2015, **7**, 1882.
31 S. Malola and H. Häkkinen, *J. Am. Chem. Soc*., 2019, **141**, 6006.
32 H. Huo and M. Rupp, arXiv.org/1704.06439v3.
33 K. Hirata et al., *Nanoscale*, 2017, **9**, 13409
34 K. Hirata et al., *Phys. Chem. Chem. Phys*., 2019, **21**, 17463.
35 K. Kim et al., *Angew. Chemie Int. Ed*., 2019, **58**, 11637.
36 K. Hirata et al., *J. Phys. Chem. C*, 2019, **123**, 13174.
37 A.P. Veenstra et al., *J. Phys. Chem. Lett.,* 2020, **11**, 2675.
38 Y. Tasaka, K. Nakamura, S. Malola, K. Hirata, K. Kim, K. Koyasu, H. Häkkinen and T. Tsukuda, *J. Phys. Chem. Lett*., 2020, **11**, 3069.
39 L.A. Angel, L.T. Majors, A.C. Dharmaratne and A. Dass, *ACS Nano*, 2010, **8**, 4691.
40 T. Dainese et al., *ACS Nano*, 2014, **8**, 3904.

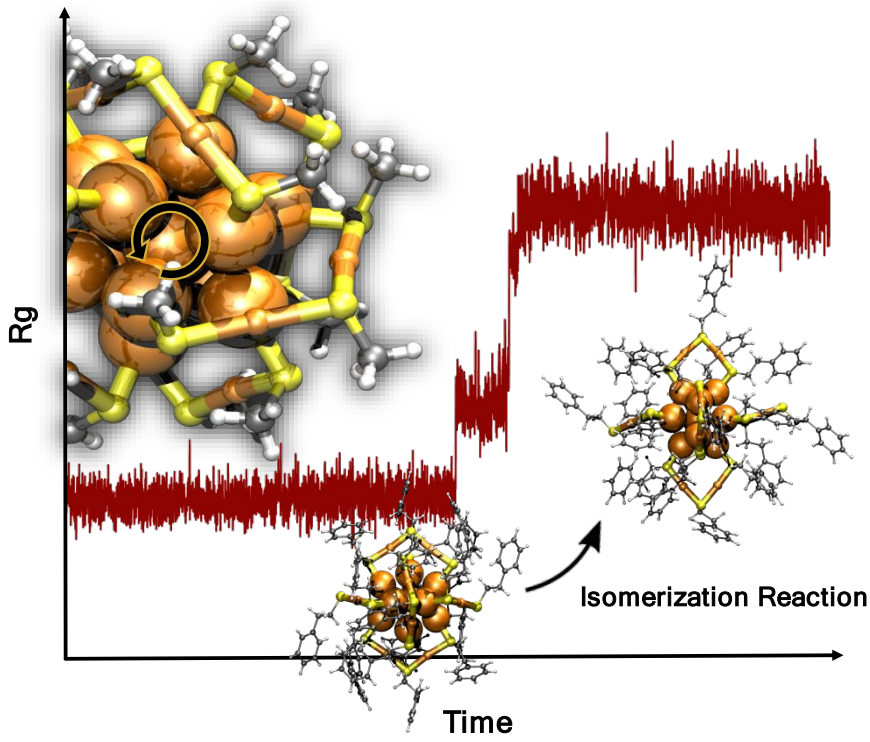

Computer simulations predict an isomer of the well-known thiolate-stabilized $Au_{25}(SR)_{18}^-$ cluster that is isoenergetic to the known structure and is topologically connected via a low-energy barrier.